Technical Note: Do different projections matter for the Budyko framework?

Remko C. Nijzink[1] and Stanislaus J. Schymanski[1]

[1]Catchment and Ecohydrology Group (CAT), Environmental Research and Innovation (ERIN), Luxembourg Institute of Science and Technology (LIST), Belvaux, Luxembourg

Correspondence: remko.nijzink@list.lu

Abstract. The widely used Budyko framework defines the water- and energy-limits of catchments. Generally, catchments plot close to these physical limits and Budyko (1974) developed a curve that predicted the positions of catchments in this framework. ~~The original formulation of the curve had no parameters, but later a more general, parameterized form was adopted. Originally, Budyko defined~~ Often, the independent variable is defined as an aridity index ~~with the potential evaporation divided by the precipitation (E_p/P) and used this~~, which is used to predict the ratio of actual evaporation over precipitation (E_a/P). However, the framework can be formulated ~~in different ways and others defined the framework~~ with the potential evaporation as the common denominator for the dependent and independent variables, i.e. P/E_p and E_a/E_p. It is possible to mathematically convert between these formulations, but if the parameterized Budyko curves are fit to data, the different formulations could lead to differences in the resulting parameter values. Here, we tested this for 357 catchments across the contiguous United States. ~~This was done by fitting a parameterized form of the curve for the two different formulations.~~

In this way, we found that differences in n-values due to the used projection could be +/- 0.2. If robust fitting algorithms were used ~~, instead of a linear least squares algorithm,~~ the differences in n-values reduced, but were nonetheless still present. The distances to the curve, often used as a metric in Budyko-type analyses, systematically ~~dependended~~ depended on the projection, with larger differences for the ~~side~~ non-contracted sides of the framework ~~with $E_p/P > 1$ for a projection with a dryness index and $P/E_p > 1$ for a projection with a wetness index~~ (i.e. ~~the non-contracted sides od the framework~~ $E_p/P > 1$ or $P/E_p > 1$). When using the two projections for predicting E_a, we found that uncertainties due to the used projections could exceed 1.5%. An important reason for the differences in n-values, curves and resulting estimates of E_a could be found in datapoints that clearly appear as outliers in one projection, but less so in the other projection.

We argue here that the non-contracted side of the framework in the two projections should always be assessed, especially for datapoints that appear as outliers. At least, one should consider the additional uncertainty of the projection and assess the robustness of the results in both projections.

1 Introduction

Budyko (1974) defined the water- and energy-limits of catchments in a simple framework and found that most catchments plot close to these limits. He defined a curve through these observations, which is known as the Budyko curve. The framework and

25 curve are widely applied and the original work of Budyko (1974) has been cited over 3100 times (google scholar). Besides that, Budyko's approach finds itself currently in a renaissance, as can be noted by the large number of studies related to the Budyko framework over the recent years. The strength of the approach is widely acknowledged, and especially its simplicity is appealing.

~~Originally, Budyko took the arithmetic mean of the curves~~ Even though often referred to as the Budyko framework, the base
30 of the framework was formed by the work of Ol'Dekop (1911) and Schreiber (1904). Initially, Schreiber (1904) formulated an exponential function to calculate the runoff ratio of a catchment, but only as a function of precipitation and a constant, catchment specific parameter. Ol'Dekop (1911) added evaporation to this equation, but also formulated his own hyperbolic tangent function. Budyko (1974) took later the arithmetic mean of the exponential function and the hyperbolic tangent function, which both had no parameters to adjust the curve. This was changed by Turc (1954) in France and independently in the Soviet
35 Union by Mezentsev (1955), who both introduced an adjustable exponent ~~α~~. This parameterized form was adopted later by others, in more general formulations ~~from for example~~, e.g. Fu (1981), Zhang et al. (2001) and Roderick and Farquhar (2011). These formulations often use one single parameter to adjust the curve to the observations. ~~Moreover, it has been argued that this parameter is~~ See also Andréassian and Sari (2019) for more details about the historical perspective.

More recently, the Budyko framework has gained popularity with several studies that use the framework for water balance
40 assessment (e.g. Andréassian and Perrin, 2012; Coron et al., 2015), model constraining (e.g. Nijzink et al., 2018; Hulsman et al., 2018; M or the assessment of climate change effects (e.g. van der Velde et al., 2014; Bouaziz et al., 2022). In addition, several studies exist that adjust the framework for different time-scales (Zhao et al., 2020; Wang et al., 2022) or different application fields (Sankarasubramanian et al., 2020).

A large number of studies considers the parameter in the Budyko framework as catchment specific and ~~that it~~ a function
45 of local catchment characteristics. It has been argued that this parameter explains local climatic and environmental conditions ~~(e.g. Oudin et al., 2008; Yang et al., 2009; Roderick and Farquhar, 2011; Donohue et al., 2012).~~

~~In order to determine the appropriate parameter value, the curve needs to be fit, with either a climatic aridity or wetness index as independent variable.~~ combined (e.g. Roderick and Farquhar, 2011), but it is often also related to vegetation (e.g. Yang et al., 2009; Li e , land cover (Oudin et al., 2008) or human activities (Liang et al., 2015; Yang et al., 2020). Moreover, Zhang et al. (2001) defined
50 n specifically as the plant available water coefficient. In addition to vegetation, Donohue et al. (2012) related the parameter to multiple variables including storm depths and soil water storage capacities. Furthermore, seasonality is often considered as well as a factor that influences this parameter (Shao et al., 2012; Ning et al., 2017).

Budyko formulated his curve with an aridity index as the independent variable, and most other publications followed that definition. From the older and traditionally cited publications, only Turc (1954) and Pike (1964) formulated the framework with
55 potential evaporation as the common denominator and P/E_p as the independent variable Andréassian et al. (2016). Nowadays, most publications still use a form of the Budyko framework with the dryness or aridity index E_p/P to predict the dependent variable E_a/P, similar as Budyko, but a substantial number of papers uses P/E_p as independent variable to predict the ratio of E_a/E_p. Here we refer to these different ways of expressing the dependent and independent variables in the Budyko framework

60

The choice of the projection may depend on the purpose of a given study. Often, the projection with an aridity index is used as it allows for a straightforward estimation of the runoff ratio ($Q/P = 1 - E_a/P$), which can, for example be used directly for constraining hydrological models (e.g. Nijzink et al., 2018; Hulsman et al., 2018). In contrast, assessing responses to changes in precipitation may require a projection that uses E_a/E_p as the predicted variable (e.g. Dooge et al., 1999), in order to allow

65

for a clearer interpretation of sensitivities. Others use the different projections simultaneously, for example to identify gaining or leaky catchments (Andréassian and Perrin, 2012). However, a large number of studies uses the projection based on an aridity index, most likely just following the definition of the framework by Budyko (1974), without questioning the appropriateness of this projection.

Generally, the projections should not make a large difference, as the equations can be rewritten in the different formats (see

70

for example Roderick and Farquhar, 2011), but here we argue that this does matter in case the curve is fit to observations. Moreover, these different ways of defining the Budyko space may lead to different interpretations of deviations from the curve. Therefore, we explore here the consequenses of the used projection, and address the following research question:

Does the choice of the projection and fitting algorithm have a systematic influence on the curve parameter, uncertainties, distances of individual catchments to the curve or distances of individual catchments to the physical limits?

75

2 Methodology

In order to address the research question, the Budyko framework was applied to a selection of catchments accross the contiguous United States. An open science approach was followed by using the platform RENKU (https://renkulab.io/, last access: 30 March 2022), which stores all data, scripts and analyses as well as the linkage between these elements. An online repository contains all information necessary for reproducibility and repeatability (https://renkulab.io/projects/remko.nijzink/budyko, last

80

access: 30 March 2022), with the final figures and latex-files in a separate repository (https://renkulab.io/gitlab/remko.nijzink/ budyko_tech_note, last access: 4 April 2022).

2.1 Budyko formulations

The Budyko formulation adopted for our analysis was originally formulated by Mezentsev (1955) (as traced back by Yang et al., 2008), but used afterwards by, amongst others, Choudhury (1999) and Roderick and Farquhar (2011):

85
$$\overline{E_a} = \frac{\overline{E_p P}}{\left(\overline{P}^n + \overline{E_p}^{-n}\right)^{1/n}} \tag{1}$$

with $\overline{E_p}$ the mean annual potential evaporation, $\overline{E_a}$ the mean annual evaporation, $\overline{P}$ the mean annual precipitation, and n a shape factor, assumed to represent catchment characteristics (e.g. vegetation, soils).

This equation can ~~also be formulated with the fraction~~ be reformulated by dividing the left hand side and right hand side by $\overline{P}$, followed by dividing the nominator and denominator on the right hand side by $\overline{P}$ as well, leading to:

$$\frac{\overline{E_a}}{\overline{P}} = \frac{\overline{E_p}}{\overline{P}} \left(\left(\frac{\overline{E_p}}{\overline{P}} \right)^n + 1 \right)^{-1/n} \tag{2}$$

In a similar way, Equation 1 can be expressed by the ratio of $\overline{P}/\overline{E_p}$ as the dependent variable. First both sides of Equation 1 are divided by $\overline{E_p}$ again, followed by dividing the nominator and denominator on the right hand side by $\overline{E_p}$ (see also Supplement S1):

$$\frac{\overline{E_a}}{\overline{E_p}} = \frac{\overline{P}}{\overline{E_p}} \left(\left(\frac{\overline{P}}{\overline{E_p}} \right)^n + 1 \right)^{-1/n} \tag{3}$$

These two formulations are often used interchangeably, and data can be plotted in figures based on Equation 2 or 3. We will adopt here dryness index projection and wetness index projection throughout the manuscript for projections based on Equation 2 and 3, respectively, to refer to these different ways of applying the Budyko framework.

2.2 Fitting the Budyko equations

The exponent n in Equations 2 and 3 was fit to data of multiple catchments with a least squares fit based on the Levenberg-Marquard algorithm (python scipy.optimize.curve_fit, https://docs.scipy.org/doc/scipy/reference/generated/scipy.optimize.curve_fit.html, last access: 10 February 2022, Levenberg, 1944). Normally, this algorithm minimizes the sum of the squared residuals, i.e. it uses a linear least squares loss function. Afterwards, instead of using a linear least squares loss function, other loss functions to minimize the residuals were used, in order to obtain a robust fit. These loss functions $\rho(z)$ are summarized in Table 1, and the final, resulting loss function is defined as:

$$\rho' = C^2 * \rho \left(x_r{}^2 / C^2 \right) \tag{4}$$

with x_r the residual of datapoint x, C a scale parameter, ρ' the resulting loss, and $\rho()$ the loss-function (see Table 1). The scale parameter C generally separates outliers from the data and was given different values between 0.1 and 1 in order to vary the datapoints that are considered as outliers, where low values of C classify the most datapoints as outliers. Note that $C = 1$ with a linear loss function results in an ordinary least squares fit again.

2.3 CAMELS data

In order to test the different hypotheses, the CAMELS data (Addor et al., 2017; Newman et al., 2015) was used, as it provides a large dataset of 671 catchments across the contiguous United States. For each catchment in this dataset, daily discharge,

4

Table 1. Loss-functions used for fitting the Budyko curves, from https://docs.scipy.org/doc/scipy/reference/generated/scipy.optimize.curve_fit.html, last access: 10 February 2022.

Method	Equation
linear	$\rho(z) = z$
soft	$\rho(z) = 2 * ((1 + z)^{0.5} - 1)$
Huber	$\rho(z) = \begin{cases} z, & \text{if } z <= 1. \\ 2 * z^{0.5} - 1, & \text{otherwise.} \end{cases}$
Cauchy	$\rho(z) = ln(1 + z)$
Arctan	$\rho(z) = arctan(z)$

rainfall, potential evaporation and air temperature are available. Eventually, 357 catchments were selected based on several conditions similar to Gnann et al. (2019):

115
  – Positive long term mean mean discharge: $\overline{Q} >= 0$ mm/year.

  – Positive long term mean mean precipitation: $\overline{P} >= 0$ mm/year.

  – Runoff ratio smaller than unity: $\overline{Q}/\overline{P} <= 1$.

  – Long term actual evaporation may not exceed potential evaporation: 1 - $\overline{Q}/\overline{P} <= \overline{E}_p/\overline{P}$.

  – No lakes: water fraction $>= 5\%$

120
  – No snow-dominated catchments: mean elevation $<= 2000$ m and snow days $<= 20\%$.

  – Relatively large catchments: area $>= 100$ km^2.

Afterwards, the actual evaporation was determined based on the long-term waterbalance, assuming that storage change is negligible over a longer period of time:

$$\overline{E}_a = \overline{P} - \overline{Q} \tag{5}$$

125
with $\overline{P}$ the mean annual precipitation, $\overline{Q}$ the mean annual discharge, $\overline{E}_a$ the mean annual actual evaporation. In this way, all water balance components are known to plot the data in the Budyko space.

2.4 Approach

The research question was addressed by a simple approach. First, the Budyko curves were fit to the CAMELS data with the different loss-functions as defined in Sect. 2.2, in the two different projections. This was done for the selected 357 catchments

130 all together, as well as for catchments grouped by a high aridiy ($E_p/P > 1$, <u>247 catchments</u>) and a low aridity ($E_p/P <= 1$, <u>110 catchments</u>). The latter to assess whether differences start to occur when catchments are dominantly in either the contracted side of the framework (i.e. $E_p/P <= 1$ or $P/E_p >= 1$) or the non-contracted side of the framework. The vertical distances to the curve as well as the distances to the envelope of the physical limits were calculated for the different projections.

In the next step, the uncertainty in the estimated mean annual actual evaporation due to the different projections was assessed.
135 This was done by selecting one catchment for the prediction of mean annual actual evaporation, whereas the remaining 356 catchments were used to fit the Budyko curve. This was again carried out in a projection based on a wetness index and a dryness index. As both estimates can be considered equally likely, the uncertainty was defined as the relative difference from the mean of the two estimates (i.e. the difference between the estimates equals two times the uncertainty). In addition, the predictions were evaluated by the relative error compared with the water balance based observed evaporation. The procedure was repeated
140 for each catchment, leading to uncertainty estimates and relative errors for each catchment. Eventually, predictions were also made by just using the non-contracted side of the framework.

3 Results and Discussion

3.1 Fitting the Budyko curve for different projections

Fitting the selected catchments of the CAMELS dataset to the two different projections led to different values for the n-
145 exponent in Equations 2 and 3 (Figure 1a and b, n=2.254 and n=2.037 respectively). These n-values differed even stronger when the catchments were separated in two groups based on their aridity ($E_p/P > 1$ and $E_p/P <= 1$ respectively, Figure 1c and d). Especially for the energy-limited catchments ($E_p/P <= 1$, shown in red), the values changed strongly from an n-value of 2.181 in the projection with a dryness index (Figure 1c), to a value of 1.967 in the projection with a wetness index (Figure 1d). The differences that occured when the curves with the two different n-values from the two different projections were
150 used in the same projection and subtracted from each other (Figures 1e and 1f), also show that especially the curves based on energy-limited catchments strongly deviated ($E_p/P <= 1$, shown in red). In contrast, the curves obtained for water-limited catchments ($E_p/P > 1$, blue) remained more similar with negligible differences.

The results presented in Figure 1 also strongly depended on the choice of the method, which was here a linear least squares fit. Repeating the analysis with more robust methods (see Table 1) led to smaller differences between n-values in the two
155 projections, even though differences were still present (Figure 2a). Especially the scale parameter C (Equation 4) that identifies datapoints as outliers, had a strong effect on the resulting n-values when set to a larger value. Nevertheless, differences still occured for small values of this scale parameter, i.e the most stringent values that classify the most datapoints as outliers, even though these differences became relatively minor. In contrast to what was found with the linear least squares method, the robust methods resulted in differences in n-values for the water-limited catchments (Figure 2c, differences between blue
160 and red points) that are generally bigger than the differences in n-values for the the energy-limited catchments (Figure 2b, differences between blue and red points).
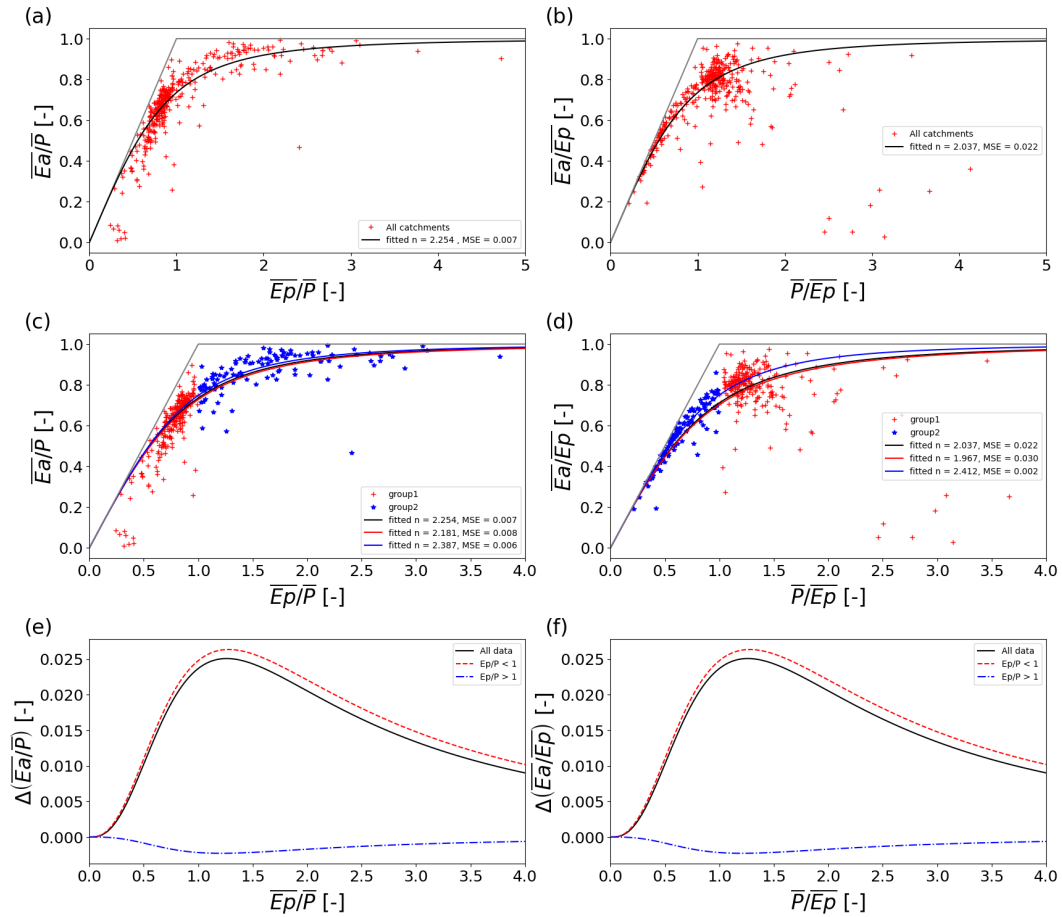
Figure 1. Camels-dataset plotted in different projections of the Budyko space, with a) and c) a projection normalized by precipitation for all catchments, b), and d) a projection normalized by potential evaporation. In c) and d) the catchments are split into two groups that are either water-limited or energy-limited, with in black the best fit curve for all catchments, in red the best fit for the group of energy-limited catchments, and in blue the best fit for the group of water-limited catchments. The differences between the curves in c) and d) are shown in e) for a projection normalized by precipitation, whereas f) shows the differences between the curves in c) and d) for a projection normalized by potential evaporation.

The above results clearly show that the projection used to fit the Budyko curve, leads to different n-values. Hence, n-values that are found by fitting Budyko-type curves, include a rather high uncertainty, and the interpretation should be carried out with care. This does not necessarily lead to large issues when n-values are considered as a ~~catchment characteristic~~ characteristic for one single catchment (e.g. Zhang et al., 2001; Donohue et al., 2012; Roderick and Farquhar, 2011), as the equations can be solved analytically when just one ~~catchment~~ data point is considered. However, ~~when multiple catchments are fit to~~ the two formulations of the curve (Equations 2 and 3) stem from the same original equation (Equation 1), meaning that the definition and value of the parameter should, in principle, not change when projections are changed. For this reason, the different values of the n-parameter found here for the different projections express an additional uncertainty due to the choice of projection. When a Budyko curve is fit to multiple catchments and the resulting n-values are used for interpretation, ~~the additional uncertainty due to the projection should be addressed~~this additional uncertainty should be considered.

3.2 Distances to the curve and envelopes

Once a Budyko curve is fit to the data, the distance to this curve is often used as a metric for catchment analysis (e.g. Potter et al., 2005; Yokoo et al., 2008; Williams et al., 2012), and supposed to tell something about the state of the catchment, catchment characteristics or the local climate. However, the distance to the curve strongly changed depending on the projection, and the differences in distances depended on the aridity of the catchments (Figure 3a). For energy-limited catchments ($E_p/P <= 1$) the distances to the curve were lower for the projection with a wetness index in comparison with the projection with a dryness index (i.e. catchments plot left of the 1:1-line in Figure 3a), whereas the opposite was true for the water-limited catchments (right of the 1:1-line in Figure 3a). This was also more generally confirmed when random samples in the Budyko space were used, see Supplement S2. The distances to the physical boundaries are less often used as a metric for catchment analysis, but these changed similarly (Figure 3b).

These findings imply as well that exchanging projections of the Budyko curve is not as straightforward as it seems, and may result in different outcomes. Moreover, different interpretations can be given to these distances, as an increased distance to $E/E_p = 1$ indicates a decreased energy use efficiency, whereas an increased distance to $E/P = 1$ indicates a decreased rain use efficiency by evaporation. In the literature, several studies focus on explaining these distances to the curve (e.g. Donohue et al., 2007, 2010; Xiong and Guo, 2012; Fang et al., 2016), rather than the n-values, but usually only consider one specific projection. Thus, one needs to be aware that these explanations are only valid for that specific projection, because the meaning as well as the value of these distances change for a different projection.

Therefore, also here a consistent use of the framework is needed. As an aridity of 1.0 introduces a clear distinction between under- and overestimating the distances to the curve and envelope in Figures 3a and b, one may consider to use only the side of the curve with $E_p/P > 1.0$ in the dryness index projection or $P/E_p < 1.0$ in the wetness index projection. In this way, the contracted side of the curve is not used, which could lead to errors due to seemingly low absolute deviations that are in relative terms clearly present.
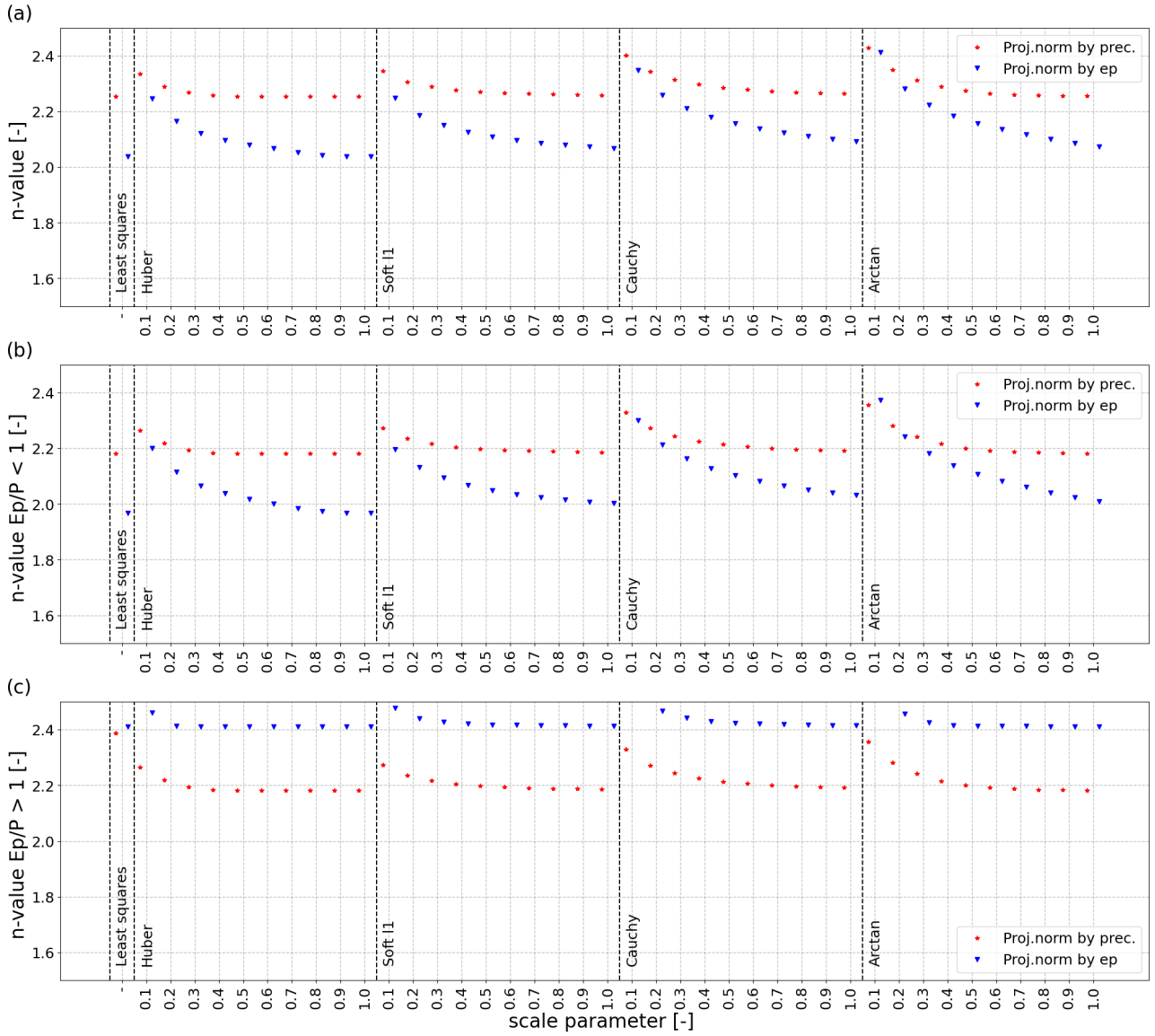
Figure 2. Fitted n-values for a) all catchments, b) energy-limited catchments and c) water-limited catchments, for projections that normalized by precipiation (blue) and potential evaporation (red). On the x-axis the different robust regression methods with different scale parameters (separating outliers from the data) are shown.
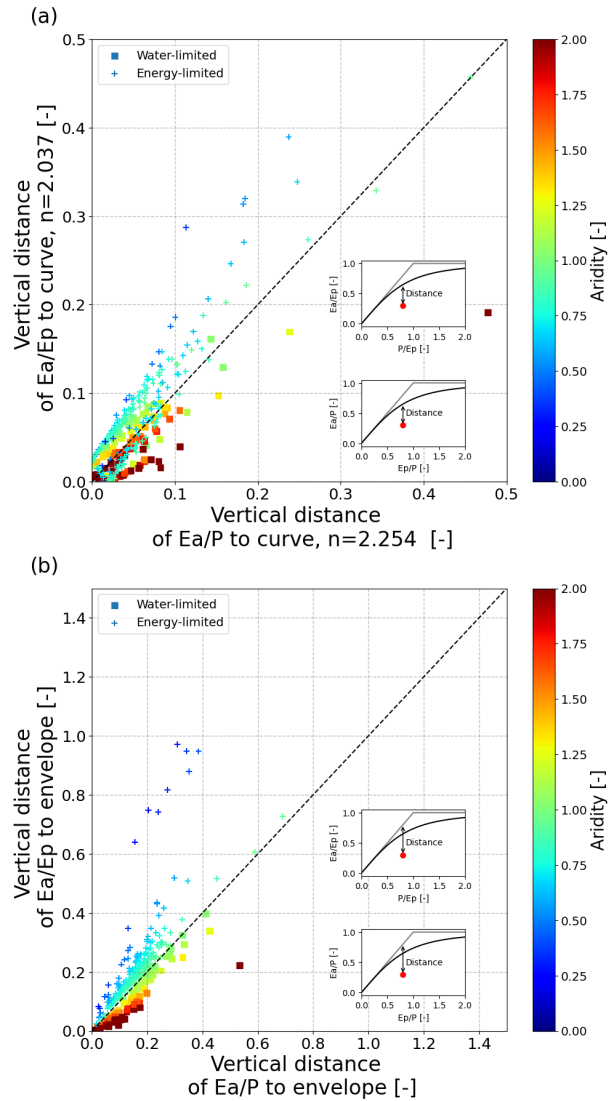
Figure 3. Vertical distances to a) the envelope of the physical limits of the Budyko framework and b) vertical distances to the fitted Budyko curve, both for projections normalized by precipitation (x-axes) and potential evaporation (y-axes). Water-limited catchments (Ep/P >1) are shown with stars, whereas energy-limited catchments are shown with crosses. The colorscale indicates the aridity of the catchments.

3.3 Uncertainty in predictions

The Budyko framework is often used to predict values of E_a for ungauged catchments, but the uncertainty in predictions of E_a due to the used projection exceeded 1.5% for catchments with an aridity around 1.0 (Figure 4a). In addition, the relative error compared with the observed E_a was especially large for energy-limited catchments of the CAMELS dataset ($E_p/P <= 1$, Figure 4b). However, the differences in the relative errors between the dryness and wetness index based estimates remained rather small (Figure 4b).

The uncertainty in predicted values of E_a due to the choice of projection in the Budyko framework has not received much attention to date. Uncertainty evaluations do exist for the Budyko framework, or derivatives thereof (e.g. Yang et al., 2014), but these studies did not consider the influence of different projections. Only Andréassian and Perrin (2012) noted that the chosen projection may lead to ambiguties, especially related to leaky or gaining catchments. Implicitly, others may include the projection-related uncertainty indirectly by defining the curves in a more statistical way (Greve et al., 2015), but we would still argue that the influence of the used projection needs more consideration.

3.4 Influence of outliers

An important cause of the different n-values in the different projections are datapoints that appear as outliers in one projection, but not in the other projection. For example, several datapoints have short vertical distances to the envelope in a dryness index projection, but have large distances to the envelope in a wetness index projection and could be considered as outliers (red points in Figure 5a and b). Vice versa, one data point appears as an outlier in a dryness index based projection (blue point in Figure 5a), but this is not apparent in the other projection (Figure 5b).

The outliers also influenced the relative errors when the curve was used to predict E_a. The group of catchments identified as outliers in a wetness index projection (i.e. red points in Figure 5), led to lower n-values with a lower curve (see also Figure 1) and a predicted E_a that is more often underestimated (blue boxes in Figure 4 shifted downwards). Once only the non-contracted side of the framework was used for predictions, the relative errors became either more negative (for $E_p/P =< 1$) or improved and approached 0 (for $E_p/P > 1$). However, this was merely a result of the absence of the group of outliers (with $E_p/P =< 1$) for the predictions of the catchments with $E_p/P > 1$. Thus, using only the contracted sides of the framework does not necessarily improve predictions of E_a. Nevertheless, we would still argue that plotting the framework in the two projections and, at least, inspecting the non-contracted sides for outliers, is a valuable and necessary step in Budyko applications.

4 Conclusions

The Budyko framework was applied to a selection of catchments across the contiguous United States, with two different ways to plot the framework. The first projection used a wetness index, whereas the second projection used a dryness index. First, curves were fit with a standard linear least squares algorithm, followed by more robust methods afterwards. Distances of
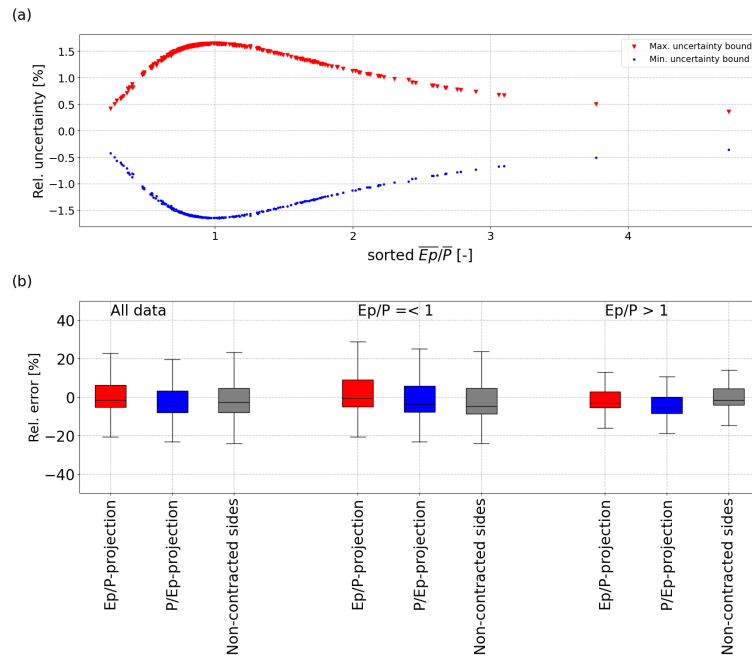
Figure 4. Uncertainty bounds of predicted values of E_a, due to different projections (a). The uncertainty is defined as the relative difference from the expected value of E_a, which is the mean of the predicted values in the two different projections. The relative errors compared with observed (water balance) E_a are shown in b) for a dryness index projection (red), a wetness index projection (blue) and when only the non-contracted sides of the framework are used (gray). Note that for the blue and red boxplots the full data is always used to derive the curve, whereas the gray boxplots only used the non-contracted side of the curve. For the gray boxplot with "All data", the non-contracted sites were used as well, i.e. the curve was fit for catchments with $E_p/P <= 1$ in a wetness index projection and for catchments with $E_p/P > 1$ in a dryness index projection.

individual catchments to the curves and envelopes were determined, in order to assess to effects of the different projections. In the next step, we assessed the uncertainty in predicted values of actual evaporation due to the different projections.

In this way, we gained the following insights:

– The differences in n-values due to the used projection were +/- 0.2 for this dataset (Figure 1).

– Robust fitting algorithms reduced the differences in n-values in the different projections, but differences were still present (Figure 2).

– The distances to the curve had a systematic dependence on the projection, with larger differences for the non-contracted side of the framework, i.e. $E_p/P > 1$ for the projection with a dryness index and $P/E_p > 1$ for the projection with a wetness index (Figure 3).

– The resulting uncertainty in predicted values of E_a, solely due to the used projections, could exceed 1.5% (Figure 4).
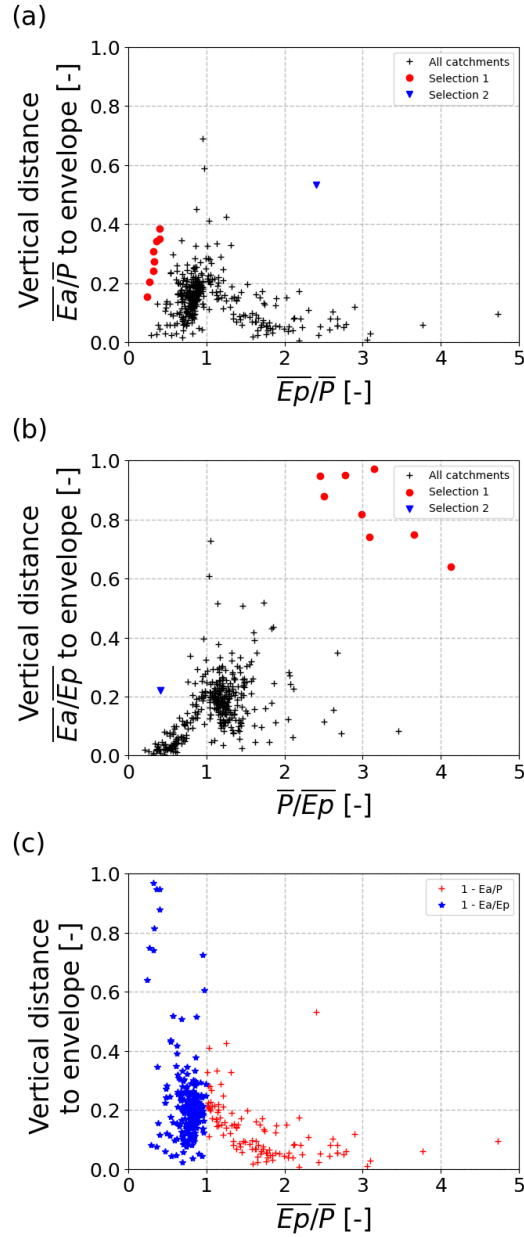
12

Figure 5. Vertical distances to the envelope for a projection with a dryness index (a) and a wetness index (b), with the same selection in catchments in blue triangles, red dots and black crosses. Distances to the envelope are shown in c) as a function of the dryness index, with in red the distances to the non-contracted side in a projection with a dryness index (i.e. $E_p/P > 1.0$ with distances $1 - E_a/P$) and in blue the distances to the non-contracted side in a projection with a wetness index (i.e. $P/E_p > 1$ with distances $1 - E_a/E_p$).

13

- Datapoints can appear as outliers in one projection, but not in the other, causing differences in the fitting of the curves (Figure 5).

These findings show that the used projection needs to be considered carefully. Here, we would like to argue to assess always the non-contracted side of the framework in the two projections. Catchments that seem close to the curve and the limits on the contracted side, can easily appear as strong outliers on the non-contracted side of the framework, as the absolute value of the relative errors changes on the x-axis on the contracted side (i.e. a 10% error in E_a/P for $E_p/P = 0.5$ differs in absolute terms for $E_p/P = 0.7$). In contrast, this does not happen when only the non-contracted side is considered. At least, it must be noted and considered that the used projection does lead to differences and adds uncertainty to analyses where Budyko curves are fit to multiple catchments. Studies that use Budyko-type curves should therefore assess whether their results are robust and remain unchanged when the projection is changed.

References

Addor, N., Newman, A. J., Mizukami, N., and Clark, M. P.: The CAMELS data set: catchment attributes and meteorology for large-sample studies, Hydrol. Earth Syst. Sci., p. 21, 2017.

Andréassian, V. and Perrin, C.: On the ambiguous interpretation of the Turc-Budyko nondimensional graph, Water Resources Research, 48, W10 601, https://doi.org/10.1029/2012WR012532, https://agupubs.onlinelibrary.wiley.com/doi/abs/10.1029/2012WR012532, 2012.

Andréassian, V. and Sari, T.: Technical Note: On the puzzling similarity of two water balance formulas – Turc–Mezentsev vs. Tixeront–Fu, Hydrology and Earth System Sciences, 23, 2339–2350, https://doi.org/10.5194/hess-23-2339-2019, https://hess.copernicus.org/articles/23/2339/2019/, 2019.

Andréassian, V., Mander, U., and Pae, T.: The Budyko hypothesis before Budyko: The hydrological legacy of Evald Oldekop, Journal of Hydrology, 535, 386–391, https://doi.org/10.1016/j.jhydrol.2016.02.002, https://linkinghub.elsevier.com/retrieve/pii/S0022169416300270, 2016.

Bouaziz, L. J. E., Aalbers, E. E., Weerts, A. H., Hegnauer, M., Buiteveld, H., Lammersen, R., Stam, J., Sprokkereef, E., Savenije, H. H. G., and Hrachowitz, M.: Ecosystem adaptation to climate change: the sensitivity of hydrological predictions to time-dynamic model parameters, Hydrology and Earth System Sciences, 26, 1295–1318, https://doi.org/10.5194/hess-26-1295-2022, https://hess.copernicus.org/articles/26/1295/2022/, 2022.

Budyko, M.: Climate and Life, Academic Press, New York and London, english Edited by Miller, D.H., 1974.

Choudhury, B.: Evaluation of an empirical equation for annual evaporation using field observations and results from a biophysical model, Journal of Hydrology, 216, 99–110, https://doi.org/10.1016/S0022-1694(98)00293-5, https://linkinghub.elsevier.com/retrieve/pii/S0022169498002935, 1999.

Coron, L., Andréassian, V., Perrin, C., and Le Moine, N.: Graphical tools based on Turc-Budyko plots to detect changes in catchment behaviour, Hydrological Sciences Journal, 60, 1394–1407, https://doi.org/10.1080/02626667.2014.964245, http://www.tandfonline.com/doi/full/10.1080/02626667.2014.964245, 2015.

Donohue, R., Roderick, M., and McVicar, T.: Can dynamic vegetation information improve the accuracy of Budyko's hydrological model?, Journal of Hydrology, 390, 23–34, https://doi.org/10.1016/j.jhydrol.2010.06.025, https://linkinghub.elsevier.com/retrieve/pii/S0022169410003604, 2010.

Donohue, R. J., Roderick, M. L., and McVicar, T. R.: On the importance of including vegetation dynamics in Budyko's hydrological model, Hydrol. Earth Syst. Sci., p. 13, 2007.

Donohue, R. J., Roderick, M. L., and McVicar, T. R.: Roots, storms and soil pores: Incorporating key ecohydrological processes into Budyko's hydrological model, Journal of Hydrology, 436-437, 35–50, https://doi.org/10.1016/j.jhydrol.2012.02.033, https://linkinghub.elsevier.com/retrieve/pii/S0022169412001461, 2012.

Dooge, J. C. I, Bruen, M., and Parmentier, B.: A simple model for estimating the sensitivity of runoff to long-term changes in precipitation without a change in vegetation, Advances in Water Resources, p. 11, 1999.

Fang, K., Shen, C., Fisher, J. B., and Niu, J.: Improving Budyko curve-based estimates of long-term water partitioning using hydrologic signatures from GRACE, Water Resources Research, 52, 5537–5554, https://doi.org/10.1002/2016WR018748, http://agupubs.onlinelibrary.wiley.com/doi/abs/10.1002/2016WR018748, _eprint: https://onlinelibrary.wiley.com/doi/pdf/10.1002/2016WR018748, 2016.

Fu, B.: On the calculation of the evaporation from land surface [in Chinese], Sci. Atmos. Sin., 5(1), 23–31, 1981.

Gnann, S. J., Woods, R. A., and Howden, N. J. K.: Is There a Baseflow Budyko Curve?, Water Resources Research, 55, 2838–2855, https://doi.org/10.1029/2018WR024464, https://onlinelibrary.wiley.com/doi/abs/10.1029/2018WR024464, 2019.

Greve, P., Gudmundsson, L., Orlowsky, B., and Seneviratne, S. I.: Introducing a probabilistic Budyko framework, Geophysical Research Letters, 42, 2261–2269, https://doi.org/10.1002/2015GL063449, https://agupubs.onlinelibrary.wiley.com/doi/abs/10.1002/2015GL063449, _eprint: https://agupubs.onlinelibrary.wiley.com/doi/pdf/10.1002/2015GL063449, 2015.

Greve, P., Burek, P., and Wada, Y.: Using the Budyko Framework for Calibrating a Global Hydrological Model, Water Resources Research, 56, e2019WR026 280, https://doi.org/10.1029/2019WR026280, http://onlinelibrary.wiley.com/doi/abs/10.1029/2019WR026280, _eprint: https://agupubs.onlinelibrary.wiley.com/doi/pdf/10.1029/2019WR026280, 2020.

Hulsman, P., Bogaard, T. A., and Savenije, H. H. G.: Rainfall-runoff modelling using river-stage time series in the absence of reliable discharge information: a case study in the semi-arid Mara River basin, Hydrology and Earth System Sciences, 22, 5081–5095, https://doi.org/10.5194/hess-22-5081-2018, https://hess.copernicus.org/articles/22/5081/2018/, 2018.

Levenberg, K.: A method for the solution of certain non-linear problems in least squares, Quarterly of Applied Mathematics, 2, 164–168, https://doi.org/10.1090/qam/10666, https://www.ams.org/qam/1944-02-02/S0033-569X-1944-10666-0/, 1944.

Li, D., Pan, M., Cong, Z., Zhang, L., and Wood, E.: Vegetation control on water and energy balance within the Budyko framework, Water Resources Research, 49, 969–976, https://doi.org/https://doi.org/10.1002/wrcr.20107, http://agupubs.onlinelibrary.wiley.com/doi/abs/10.1002/wrcr.20107, _eprint: https://onlinelibrary.wiley.com/doi/pdf/10.1002/wrcr.20107, 2013.

Liang, W., Bai, D., Wang, F., Fu, B., Yan, J., Wang, S., Yang, Y., Long, D., and Feng, M.: Quantifying the impacts of climate change and ecological restoration on streamflow changes based on a Budyko hydrological model in China's Loess Plateau, Water Resources Research, 51, 6500–6519, https://doi.org/10.1002/2014WR016589, http://onlinelibrary.wiley.com/doi/abs/10.1002/2014WR016589, _eprint: https://agupubs.onlinelibrary.wiley.com/doi/pdf/10.1002/2014WR016589, 2015.

Mezentsev, V. S.: More on the calculation of average total evaporation, Meteorol. Gidrol, 5, 1955.

Mianabadi, A., Coenders-Gerrits, M., Shirazi, P., Ghahraman, B., and Alizadeh, A.: A global Budyko model to partition evaporation into interception and transpiration, Hydrology and Earth System Sciences, 23, 4983–5000, https://doi.org/10.5194/hess-23-4983-2019, https://hess.copernicus.org/articles/23/4983/2019/, publisher: Copernicus GmbH, 2019.

Moussa, R. and Lhomme, J.-P.: The Budyko functions under non-steady-state conditions, Hydrol. Earth Syst. Sci., p. 13, 2016.

Newman, A. J., Clark, M. P., Sampson, K., Wood, A., Hay, L. E., Bock, A., Viger, R. J., Blodgett, D., Brekke, L., Arnold, J. R., Hopson, T., and Duan, Q.: Development of a large-sample watershed-scale hydrometeorological data set for the contiguous USA: data set characteristics and assessment of regional variability in hydrologic model performance, Hydrology and Earth System Sciences, 19, 209–223, https://doi.org/10.5194/hess-19-209-2015, https://www.hydrol-earth-syst-sci.net/19/209/2015/, 2015.

Nijzink, R. C., Almeida, S., Pechlivanidis, I. G., Capell, R., Gustafssons, D., Arheimer, B., Parajka, J., Freer, J., Han, D., Wagener, T., Nooijen, R. R. P. v., Savenije, H. H. G., and Hrachowitz, M.: Constraining Conceptual Hydrological Models With Multiple Information Sources, Water Resources Research, 54, 8332–8362, https://doi.org/10.1029/2017WR021895, http://agupubs.onlinelibrary.wiley.com/doi/abs/10.1029/2017WR021895, _eprint: https://onlinelibrary.wiley.com/doi/pdf/10.1029/2017WR021895, 2018.

Ning, T., Li, Z., and Liu, W.: Vegetation dynamics and climate seasonality jointly control the interannual catchment water balance in the Loess Plateau under the Budyko framework, Hydrology and Earth System Sciences, 21, 1515–1526, https://doi.org/10.5194/hess-21-1515-2017, https://hess.copernicus.org/articles/21/1515/2017/, 2017.

Ol'Dekop, E.: On evaporation from the surface of river basins, Trans. Meteorol. Obs., 4, 200, 1911.

Oudin, L., Andréassian, V., Lerat, J., and Michel, C.: Has land cover a significant impact on mean annual streamflow? An international assessment using 1508 catchments, Journal of Hydrology, 357, 303–316, https://doi.org/10.1016/j.jhydrol.2008.05.021, https://linkinghub.elsevier.com/retrieve/pii/S0022169408002345, 2008.

Pike, J.: The estimation of annual run-off from meteorological data in a tropical climate, Journal of Hydrology, 2, 116–123, https://doi.org/10.1016/0022-1694(64)90022-8, https://linkinghub.elsevier.com/retrieve/pii/0022169464900228, 1964.

Porporato, A.: Hydrology without dimensions, Hydrol. Earth Syst. Sci., p. 20, 2022.

Potter, N. J., Zhang, L., Milly, P. C. D., McMahon, T. A., and Jakeman, A. J.: Effects of rainfall seasonality and soil moisture capacity on mean annual water balance for Australian catchments, Water Resources Research, 41, W06 007, https://doi.org/10.1029/2004WR003697, http://agupubs.onlinelibrary.wiley.com/doi/abs/10.1029/2004WR003697, _eprint: https://onlinelibrary.wiley.com/doi/pdf/10.1029/2004WR003697, 2005.

Roderick, M. L. and Farquhar, G. D.: A simple framework for relating variations in runoff to variations in climatic conditions and catchment properties, Water Resources Research, 47, W00G07, https://doi.org/10.1029/2010WR009826, http://agupubs.onlinelibrary.wiley.com/doi/abs/10.1029/2010WR009826, 2011.

Sankarasubramanian, A., Wang, D., Archfield, S., Reitz, M., Vogel, R. M., Mazrooei, A., and Mukhopadhyay, S.: HESS Opinions: Beyond the long-term water balance: evolving Budyko's supply–demand framework for the Anthropocene towards a global synthesis of land-surface fluxes under natural and human-altered watersheds, Hydrology and Earth System Sciences, 24, 1975–1984, https://doi.org/10.5194/hess-24-1975-2020, https://hess.copernicus.org/articles/24/1975/2020/, 2020.

Schreiber, P.: Über die Beziehungen zwischen dem Niederschlag und der Wasserführung der Flüsse in Mitteleuropa, Z. Meteor., 21, 441–452, 1904.

Shao, Q., Traylen, A., and Zhang, L.: Nonparametric method for estimating the effects of climatic and catchment characteristics on mean annual evapotranspiration, Water Resources Research, 48, W03 517, https://doi.org/https://doi.org/10.1029/2010WR009610, http://agupubs.onlinelibrary.wiley.com/doi/abs/10.1029/2010WR009610, _eprint: https://onlinelibrary.wiley.com/doi/pdf/10.1029/2010WR009610, 2012.

Turc, L.: Calcul du bilan de l'eau: évaluation en fonction des précipitations et des températures, IAHS Publ, 37, 88–200, 1954.

van der Velde, Y., Vercauteren, N., Jaramillo, F., Dekker, S. C., Destouni, G., and Lyon, S. W.: Exploring hydroclimatic change disparity via the Budyko framework, Hydrological Processes, 28, 4110–4118, https://doi.org/10.1002/hyp.9949, http://onlinelibrary.wiley.com/doi/abs/10.1002/hyp.9949, _eprint: https://onlinelibrary.wiley.com/doi/pdf/10.1002/hyp.9949, 2014.

Wang, F., Xia, J., Zou, L., Zhan, C., and Liang, W.: Estimation of time-varying parameter in Budyko framework using long short-term memory network over the Loess Plateau, China, Journal of Hydrology, 607, 127 571, https://doi.org/10.1016/j.jhydrol.2022.127571, https://linkinghub.elsevier.com/retrieve/pii/S0022169422001469, 2022.

Williams, C. A., Reichstein, M., Buchmann, N., Baldocchi, D., Beer, C., Schwalm, C., Wohlfahrt, G., Hasler, N., Bernhofer, C., Foken, T., Papale, D., Schymanski, S., and Schaefer, K.: Climate and vegetation controls on the surface water balance: Synthesis of evapotranspiration measured across a global network of flux towers, Water Resources Research, 48, W06 523, https://doi.org/10.1029/2011WR011586, http://www.agu.org/pubs/crossref/2012/2011WR011586.shtml, 2012.

Xiong, L. and Guo, S.: Appraisal of Budyko formula in calculating long-term water balance in humid watersheds of southern China, Hydrological Processes, 26, 1370–1378, https://doi.org/10.1002/hyp.8273, http://onlinelibrary.wiley.com/doi/abs/10.1002/hyp.8273, _eprint: https://onlinelibrary.wiley.com/doi/pdf/10.1002/hyp.8273, 2012.

Yang, D., Shao, W., Yeh, P. J.-F., Yang, H., Kanae, S., and Oki, T.: Impact of vegetation coverage on regional water balance in the nonhumid regions of China, Water Resources Research, 45, W00A14, https://doi.org/10.1029/2008WR006948, http://agupubs.onlinelibrary.wiley.com/doi/abs/10.1029/2008WR006948, _eprint: https://onlinelibrary.wiley.com/doi/pdf/10.1029/2008WR006948, 2009.

365 Yang, H., Yang, D., Lei, Z., and Sun, F.: New analytical derivation of the mean annual water-energy balance equation, Water Resources Research, 44, W03 410, https://doi.org/10.1029/2007WR006135, http://agupubs.onlinelibrary.wiley.com/doi/abs/10.1029/2007WR006135, _eprint: https://onlinelibrary.wiley.com/doi/pdf/10.1029/2007WR006135, 2008.

Yang, H., Yang, D., and Hu, Q.: An error analysis of the Budyko hypothesis for assessing the contribution of climate change to runoff, Water Resources Research, 50, 9620–9629, https://doi.org/https://doi.org/10.1002/2014WR015451, http://agupubs.onlinelibrary.wiley.com/doi/abs/10.1002/2014WR015451, _eprint: https://onlinelibrary.wiley.com/doi/pdf/10.1002/2014WR015451, 2014.

370 Yang, H., Xiong, L., Xiong, B., Zhang, Q., and Xu, C.-Y.: Separating runoff change by the improved Budyko complementary relationship considering effects of both climate change and human activities on basin characteristics, Journal of Hydrology, 591, 125 330, https://doi.org/10.1016/j.jhydrol.2020.125330, https://linkinghub.elsevier.com/retrieve/pii/S0022169420307903, 2020.

Yokoo, Y., Sivapalan, M., and Oki, T.: Investigating the roles of climate seasonality and landscape characteristics on mean annual and monthly water balances, Journal of Hydrology, 357, 255–269, https://doi.org/10.1016/j.jhydrol.2008.05.010, https://linkinghub.elsevier.com/retrieve/pii/S0022169408002278, 2008.

375 Zhang, L., Dawes, W. R., and Walker, G. R.: Response of mean annual evapotranspiration to vegetation changes at catchment scale, Water Resources Research, 37, 701–708, https://doi.org/10.1029/2000WR900325, http://agupubs.onlinelibrary.wiley.com/doi/abs/10.1029/2000WR900325, _eprint: https://onlinelibrary.wiley.com/doi/pdf/10.1029/2000WR900325, 2001.

Zhao, J., Huang, S., Huang, Q., Leng, G., Wang, H., and Li, P.: Watershed water-energy balance dynamics and their association with diverse influencing factors at multiple time scales, Science of The Total Environment, 711, 135 189, https://doi.org/10.1016/j.scitotenv.2019.135189, https://linkinghub.elsevier.com/retrieve/pii/S0048969719351812, 2020.